What we've been up to beyond k-eff at LLNL

Presented at the Technical Meeting on the Compilation of Nuclear Data Experiments for Radiation Characterization (CoNDERC)
10-14 October 2022 at IAEA, Vienna, Austria

Dave Heinrichs
Tim Classen
Soon Kim
Ed Lent
Daniel Siefman
Lucas Snyder

October 1, 2022

LLNL-PRES-840877
This work was performed under the auspices of the U.S. Department of Energy by Lawrence Livermore National Laboratory under contract DE-AC52-07NA27344. Lawrence Livermore National Security, LLC

Lawrence Livermore National Laboratory

Compilation of Nuclear Data Experiments for Radiation Characterisation (CoNDERC)

Test, Verification, or Validation Suite	Type	Number of Cases	Documentation
Regression tests	Test	11 cases	
NRF tests	Test	3 cases	
Analytic benchmarks	Verification	107 cases	LLNL-TR-648225
β-eff benchmarks	Validation	20 cases	LLNL-PRES-796197
SINBAD shielding benchmarks	Validation	9 cases	UCRL-TR-202654
KSU Co-60 silo skyshine shielding benchmarks	Validation	27 cases	UCRL-TR-202654
KSU Cs-137 air-over-ground/concrete shielding benchmarks	Validation	9 cases	LLNL-TR-838835
SILENE activation benchmarks • Unreflected • Reflected by Cd-lined CH2 • Reflected by Pb	Validation	11 cases	• ORNL/TM-2015/426 Rev. 1 • ORNL/TM-2016/317 • ORNL/TM-2016/316
Photonuclear benchmarks	Validation	16 cases	UCRL-CONF-200552
^{252}Cf spectrum average cross sections and spectral indices	Validation	16 cases 11 cases	LLNL-TR-836050
BR-1 reactor spectral indices benchmarks	Validation	38 cases	LLNL-TR-838379
Spectral Indices Benchmarks for Nine Los Alamos Fast Critical Assemblies: Godiva, Flattop-25, Big Ten, Jezebel, Flattop-Pu, Thor, Jezebel-23, Flattop-23, and Dirty Jezebel	Validation	60 cases	LLNL-TR-839692
ICSBEP criticality benchmarks	Validation	3,395 cases	• LLNL-CONF-838004 • LLNL-MI-838253

A significant effort is on-going at LLNL to document COG benchmark results with reports available at:

https://cog.llnl.gov

IAEA NDS is welcome to incorporate this work into CoNDERC.

Table A-1. COG 11.3 calculated beta-eff results (in pcm) with ENDF/B-VIII.0

	Assembly	Experiment	β_{eff} = Fissions by delayed neutrons divided by all fissions		β_{eff} = Neutrons from fissions by delayed neutrons divided by neutrons from all fissions		β_{eff} = 1 – (k-prompt/k-eff)	
No.	Name	β_{eff}	β_{eff}	C/E	β_{eff}	C/E	β_{eff}	C/E
1	NASA ZPR-1 H/X=190	900 ± 60	844	0.938 ± 6.7%	844	0.938 ± 6.7%	844 ± 2	0.938 ± 6.7%
2	NASA ZPR-1 H/X=473	860 ± 50	806	0.937 ± 5.8%	805	0.936 ± 5.8%	805 ± 1	0.936 ± 5.8%
3	NASA ZPR-1 H/X=565	820 ± 40	794	0.968 ± 4.9%	794	0.968 ± 4.9%	794 ± 1	0.968 ± 4.9%
4	TCA 1.50U 19x19	771 ± 18	772	1.001 ± 2.3%	765	0.992 ± 2.3%	763 ± 6	0.990 ± 2.5%
5	TCA 1.83U Cylinder	771 ± 17	771	1.000 ± 2.2%	766	0.994 ± 2.2%	763 ± 5	0.990 ± 2.3%
6	TCA 1.83U 17x17	766 ± 18	770	1.005 ± 2.4%	764	0.997 ± 2.4%	762 ± 5	0.995 ± 2.4%
7	TCA 2.48U 16x16	765 ± 18	764	0.999 ± 2.4%	759	0.992 ± 2.4%	757 ± 5	0.988 ± 2.4%
8	SNEAK 9C1	758 ± 24	727	0.959 ± 3.2%	706	0.931 ± 3.2%	700 ± 4	0.923 ± 3.2%
9	IPEN/MB-01	750 ± 4	748*	0.997 ± 0.6%	744*	0.992 ± 0.6%	743 ± 38	0.991 ± 5.1%
10	TCA 3.00U 15x15	749 ± 17	758*	1.012 ± 2.3%	754*	1.007 ± 2.3%	752 ± 5	1.004 ± 2.4%
11	FCA XIX-1	742 ± 24	737	0.993 ± 3.2%	725	0.977 ± 3.2%	723 ± 5	0.974 ± 3.3%
12	BFS-73-1	735 ± 13	735	1.000 ± 1.8%	715	0.973 ± 1.8%	710 ± 8	0.966 ± 2.1%
13	U9	731 ± 15	734	1.004 ± 2.1%	705	0.964 ± 2.1%	696 ± 4	0.952 ± 2.1%
14	Masurca R2	721 ± 11	738	1.024 ± 1.5%	719	0.997 ± 1.5%	715 ± 21	0.992 ± 3.3%
15	Big Ten	720 ± 7	729	1.013 ± 1.0%	699	0.971 ± 1.0%	688 ± 4	**0.956** ± 1.1%
16	U/Fe (ZPR9/34)	671 ± 14	687	1.024 ± 2.1%	683	1.018 ± 2.1%	683 ± 8	1.018 ± 2.4%
17	Topsy (25 Flattop)	665 ± 13	658	0.989 ± 2.0%	625	0.940 ± 2.0%	617 ± 7	**0.928** ± 2.3%
18	Godiva	659 ± 28	679	1.030 ± 4.2%	647	0.982 ± 4.2%	642 ± 4	0.974 ± 4.3%
19	OR Sphere Config. 1	657 ± 9	680	1.035 ± 1.4%	648	0.986 ± 1.4%	643 ± 4	0.979 ± 1.5%
20	OR Sphere Config. 2	657 ± 9	679	1.033 ± 1.4%	646	0.983 ± 1.4%	641 ± 4	0.976 ± 1.5%
21	SNEAK 7B	429 ± 22	414	0.965 ± 5.1%	410	0.956 ± 5.1%	406 ± 6	0.946 ± 5.3%
22	SNEAK 9C2	426 ± 19	381	0.894 ± 4.5%	374	**0.878** ± 4.5%	371 ± 6	**0.871** ± 4.7%
23	SNEAK 7A	395 ± 22	368	0.932 ± 5.6%	362	0.916 ± 5.6%	359 ± 6	0.909 ± 5.8%
24	C Ref (ZPPR21B)	384 ± 8	366	0.953 ± 2.1%	354	**0.922** ± 2.1%	353 ± 28	0.919 ± 8.2%
25	FCA XIX-2	364 ± 9	372	1.022 ± 2.5%	366	1.005 ± 2.5%	364 ± 8	1.000 ± 3.3%
26	23 Flattop	360 ± 9	359	0.997 ± 2.5%	340	0.944 ± 2.5%	336 ± 8	0.933 ± 3.5%
27	Masurca Zona 2	349 ± 6	343	0.983 ± 1.7%	338	0.968 ± 1.7%	336 ± 22	0.963 ± 6.8%
28	Skidoo (Jezebel 23)	290 ± 10	311	1.072 ± 3.4%	294	1.014 ± 3.4%	294 ± 4	1.014 ± 3.7%
29	Popsy (49 Flattop)	276 ± 7	272	0.986 ± 2.5%	259	0.938 ± 2.5%	256 ± 9	0.928 ± 4.3%
30	FCA XIX-3	251 ± 4	258	1.028 ± 1.6%	254	1.012 ± 1.6%	253 ± 7	1.008 ± 3.2%
31	P/C/SST (ZPR6-10)	223 ± 5	230	1.031 ± 2.2%	228	1.022 ± 2.2%	227 ± 8	1.018 ± 4.2%
32	Jezebel	195 ± 10	197	1.010 ± 5.1%	184	0.944 ± 5.1%	183 ± 5	0.938 ± 5.8%

*The COG calculational uncertainty in β_{eff} is ± 1 pcm in these cases. Cases highlighted in **RED** have $|C/E-1| > 3\sigma$.

Three new β-eff estimators in COG are available in <u>one</u> run as prompt and delayed neutrons and gammas are treated as separate particles until the end.

Results using JEFF-3.3 are in progress.

https://cog.llnl.gov

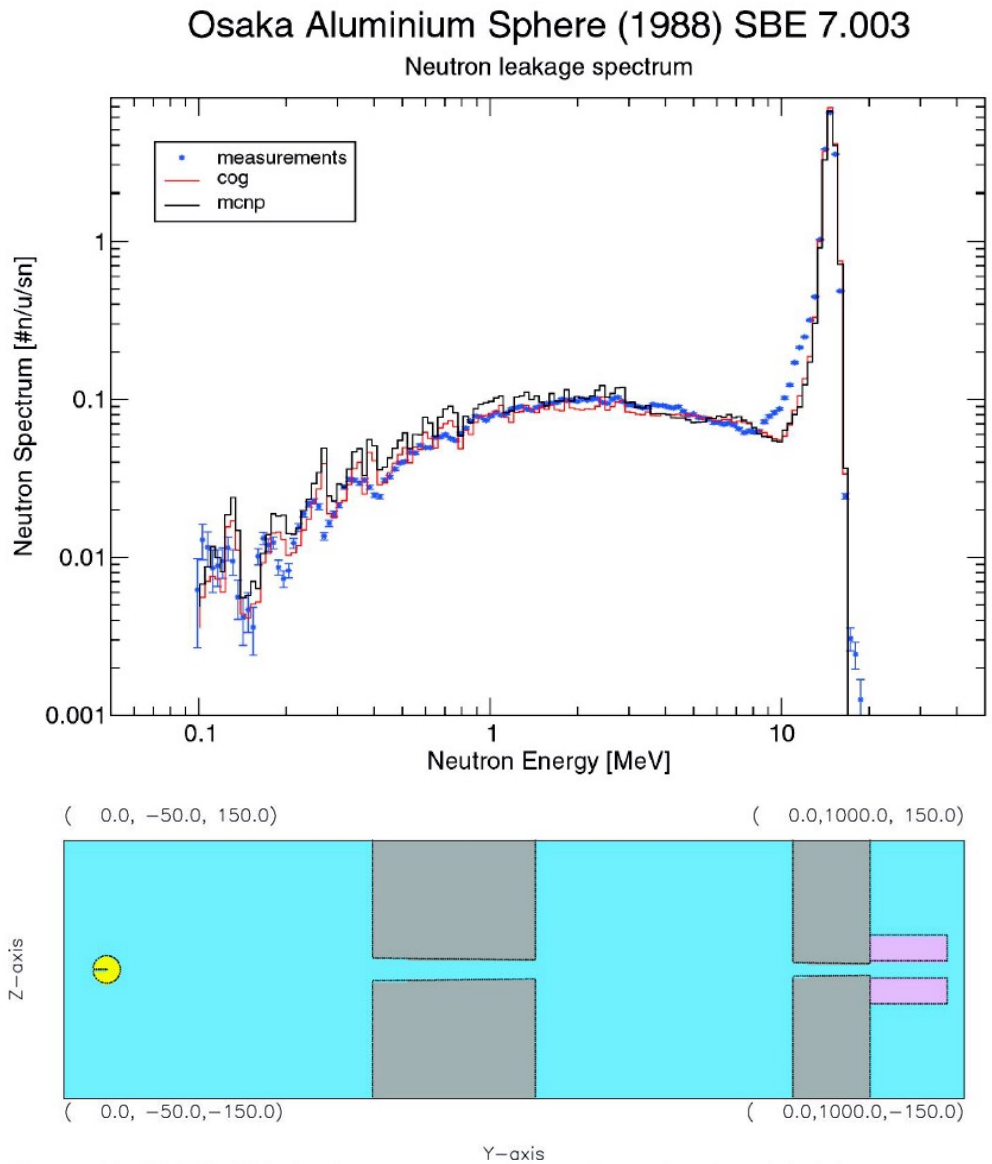

Figure 1.b OSAKA Nickel sphere geometry: Three-dimensional model of the experiment. The nickel sphere is represented in yellow, concrete walls in gray, the polyethylene collimator in pink, and air in blue. The point source is located at the center of the sphere, and the point detector is behind the collimator.

We are expanding our suite of SINBAD benchmarks beyond OKTAVIAN (M.-A. Descalle *et al.*)

https://cog.llnl.gov

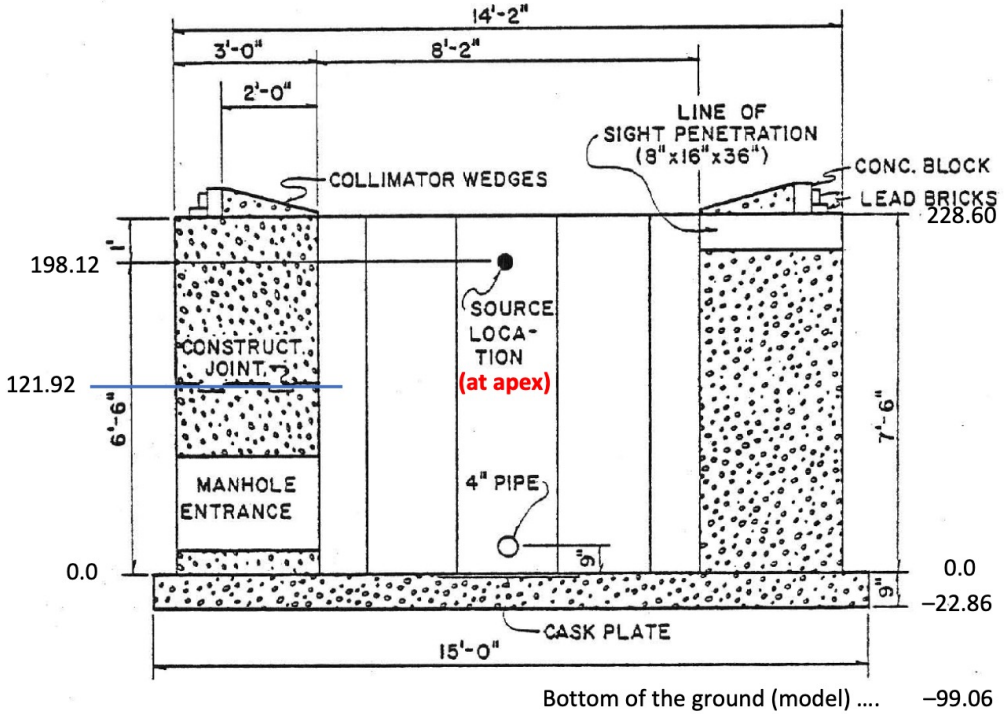

Results: Uncovered source collimated to a vertical 150.5° cone

Experiment						COG		
r (m)	ρ* (mg/cc)	ρr (g/cm²)	Source** (Ci)	Exposure Rate (μR/hr)	Exposure Rate (μR/hr•Ci)	Exposure Rate (R/s•Ci)	Exposure Rate (μR/hr•Ci)	C/E***
50	1.096	5.48	10.33	284.0 ± 0.4	27.49 ± 0.04	7.019E-9 ± 0.4%	25.27 ± 0.4%	0.92 ± 5.0%
100	1.096	10.96	10.33	113.3 ± 0.7	10.97 ± 0.07	2.695E-9 ± 0.4%	9.70 ± 0.4%	0.88 ± 5.1%
200	1.096	21.92	10.33	28.1 ± 0.4	2.72 ± 0.04	7.326E-10 ± 0.6%	2.64 ± 0.6%	0.97 ± 5.2%
300	1.096	32.88	229.1	193.0 ± 0.9	0.842 ± 0.004	2.397E-10 ± 0.3%	0.863 ± 0.3%	1.02 ± 5.1%
400	1.096	43.84	229.1	78.0 ± 0.4	0.340 ± 0.002	9.520E-11 ± 0.4%	0.343 ± 0.4%	1.01 ± 5.1%
500	1.096	54.80	229.1	29.3 ± 0.6	0.128 ± 0.003	4.099E-11 ± 0.5%	0.148 ± 0.5%	1.15 ± 5.5%
600	1.096	65.76	3804	225.0 ± 0.4	0.0591 ± 0.0001	1.782E-11 ± 0.7%	0.0642 ± 0.7%	1.09 ± 5.2%
700	1.096	76.72	3804	101.0 ± 0.9	0.0266 ± 0.0002	8.148E-12 ± 0.9%	0.0293 ± 0.9%	1.10 ± 5.1%

* 2% uncertainty in air density (negligible).
** 5% uncertainty in source strength.
*** Also includes the uncertainty in the exposure rate due to the uncertainty in detector position (see App. A).

Many benchmarks are useful for specific applications rather than nuclear data evaluation.

KSU skyshine benchmark

https://cog.llnl.gov

Dimensions: R-Z model details

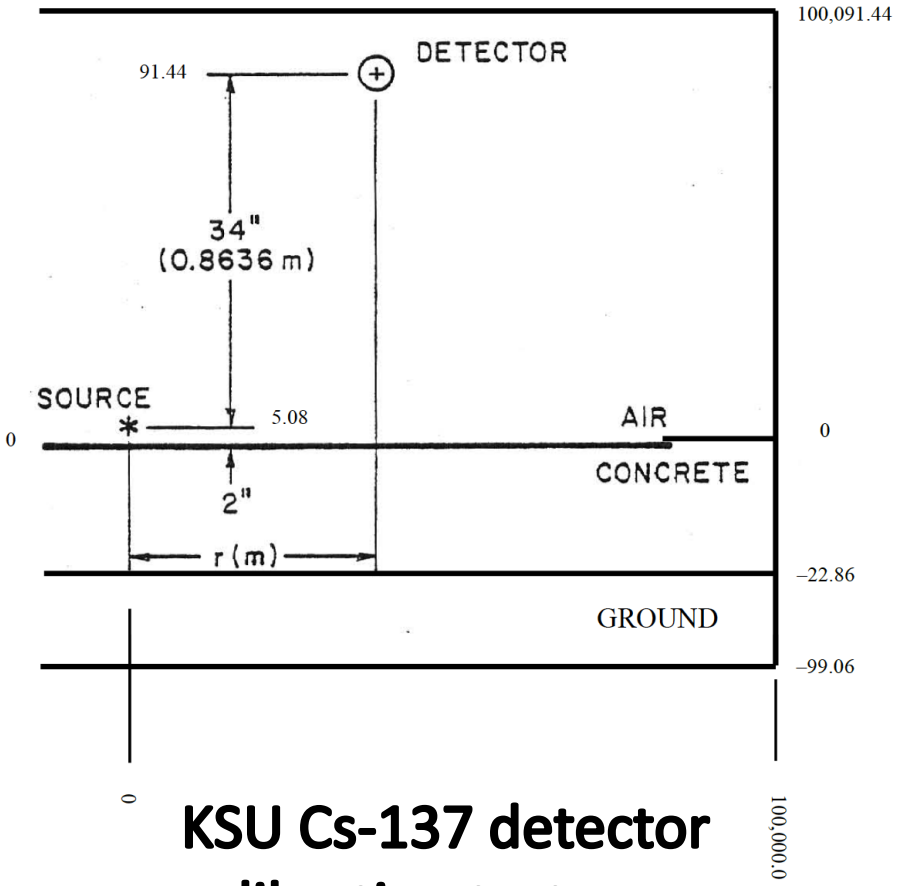

Table 6. Results for Photon Transport in Dry Air (file: ksu0)

Experiment						COG		
r (m)	ρ* (mg/cc)	ρr (g/cm^2)	Source** (mCi)	Exposure Rate (μR/hr)	Exposure Rate (μR/hr•mCi)	Exposure Rate (R/s•mCi)	Exposure Rate (μR/hr•mCi)	C/E
2	1.142	2.28	3.094	246.8 ± 0.8	79.77 ± 0.26	2.543E-8 ± 0.1%	91.54 ± 0.1%	1.15 ± 3.5%
4	1.142	4.57	14.22	320.3 ± 0.7	22.53 ± 0.05	7.117E-9 ± 0.1%	25.62 ± 0.1%	1.14 ± 3.5%
5	1.142	5.71	14.22	208.8 ± 0.8	14.68 ± 0.06	4.580E-9 ± 0.1%	16.49 ± 0.1%	1.12 ± 3.5%
7	1.142	7.99	14.22	105.8 ± 0.8	7.44 ± 0.06	2.317E-9 ± 0.1%	8.34 ± 0.1%	1.12 ± 3.6%
8	1.142	9.14	14.22	79.8 ± 0.6	5.62 ± 0.04	1.762E-9 ± 0.1%	6.34 ± 0.1%	1.13 ± 3.6%
10	1.142	11.42	14.22	53.8 ± 0.8	3.78 ± 0.06	1.114E-9 ± 0.1%	4.01 ± 0.1%	1.06 ± 3.8%
12	1.142	13.70	14.22	35.3 ± 0.6	2.48 ± 0.04	7.636E-10 ± 0.2%	2.75 ± 0.1%	1.11 ± 3.9%
14	1.142	15.99	14.22	25.7 ± 0.6	1.81 ± 0.04	5.531E-10 ± 0.2%	1.99 ± 0.2%	1.10 ± 4.1%
18	1.142	20.56	14.22	14.1 ± 0.6	0.99 ± 0.04	3.273E-10 ± 0.2%	1.18 ± 0.2%	1.19 ± 5.3%

* 2% error in air density (negligible).
** 3.5% error in source strength.

KSU Cs-137 detector calibration tests.

https://cog.llnl.gov

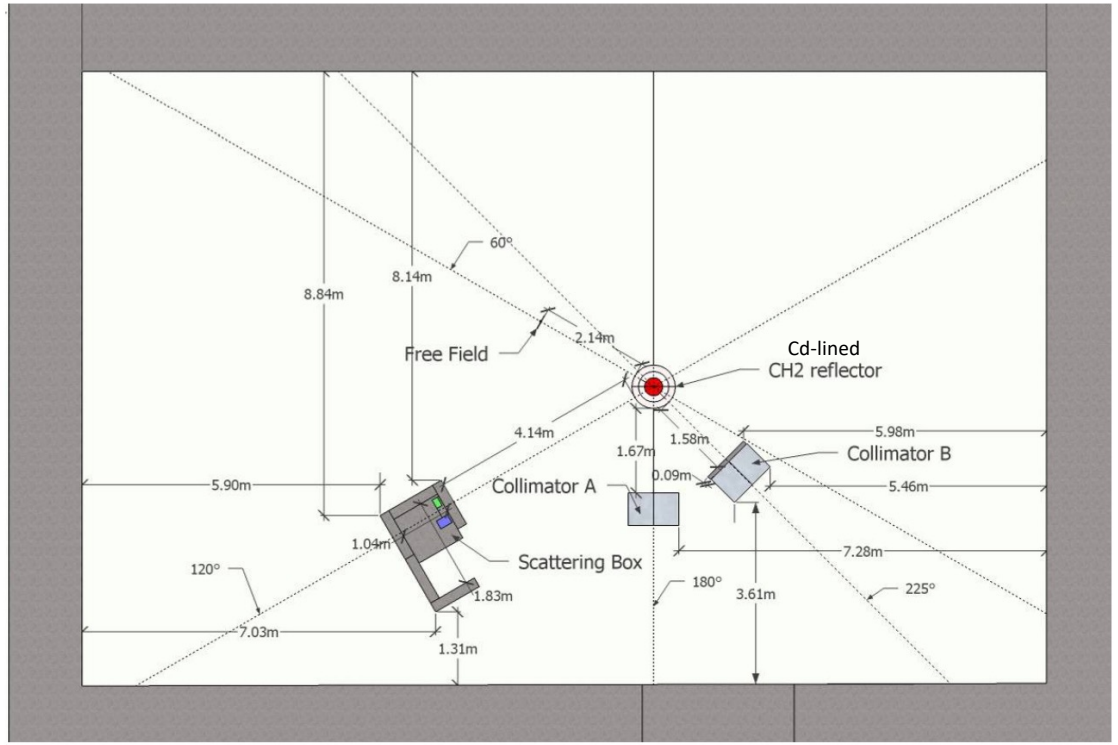

ALARM-TRAN-CH2-SHIELD-001	Neutron Activation Foil and Thermoluminescent Dosimeter Responses to a Polyethylene Reflected Pulse of the CEA Valduc Silene Critical Assembly

This SILENE neutron activation foil and photon TLD benchmark revealed no radiative capture gamma production in ENDF/B-VIII.0 for Cd isotopes. #&@!

https://cog.llnl.gov

Benchmark		Sample Calculations (C/E)			
Position	TLD (Gy) (Al_2O_3)	ENDF/B-VII.1 (MCNP)	JEF-3.1.2 (Tripoli)	ENDF/B-VII.1[a] (COG)	ENDF/B-VIII.0[b] (COG)
Collimator A	5.29 ± 8%	0.63 ± 8%	0.92 ± 8%	0.85 ± 10%	0.90 ± 9%
Collimator B	3.15 ± 8%	0.60 ± 8%	0.92 ± 9%	0.82 ± 9%	0.85 ± 12%
Free Field	4.79 ± 9%	0.65 ± 9%	0.81 ± 9%	0.90 ± 9%	0.95 ± 11%
Scattering Box 3	1.01 ± 8%	0.66 ± 8%	0.92 ± 8%	0.93 ± 9%	0.94 ± 12%
Scattering Box 4	1.14 ± 8%	0.66 ± 8%	0.87 ± 8%	0.95 ± 9%	0.99 ± 11%
	Table 3-32	Table 4-9	Table 4-13	Table 4-17	This work

Notes:

[a] Except JEFF-3.1.2 for all Cadmium isotopes.

[b] Except Belgya EXFOR data for Cd-113 and JEFF-3.3 for all other Cd isotopes.

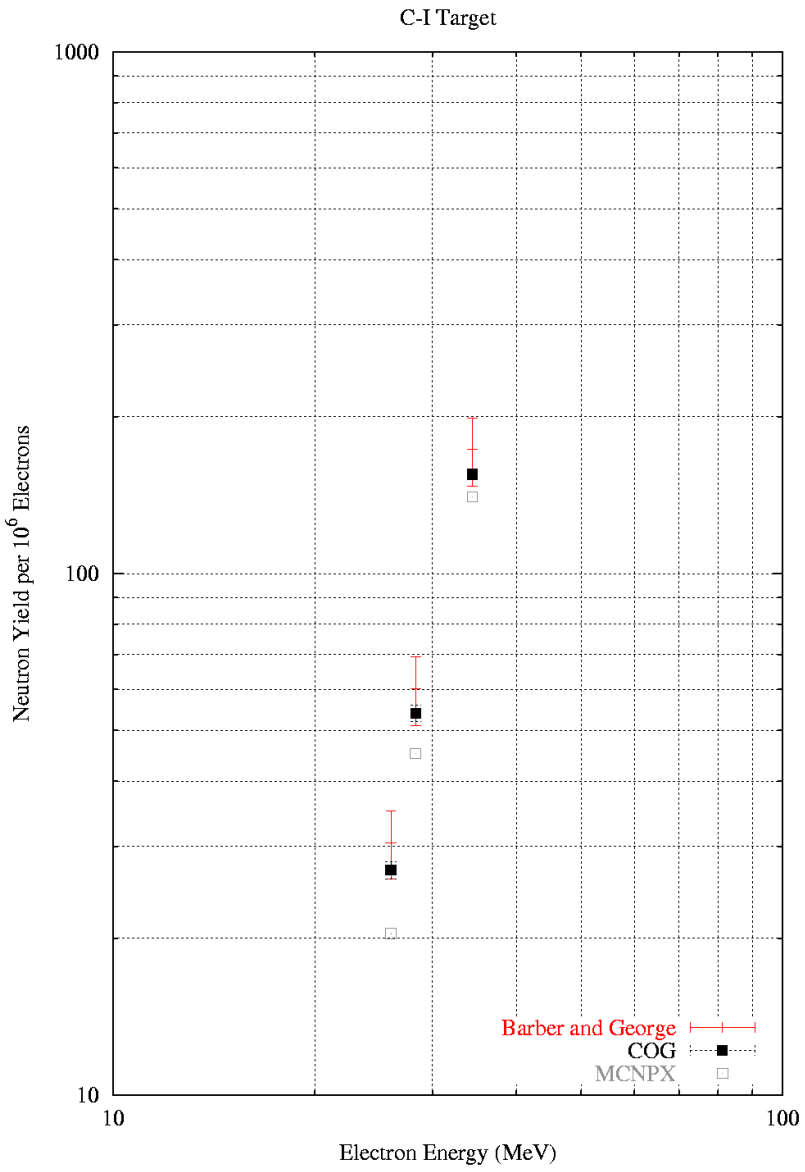

Barber and George (SLAC) photoneutron benchmarks (coupled e-γ-n problems)

Plan to redo now that COG has EGS5 inside and in-line PEGS library creation.

https://cog.llnl.gov

Table 1. COG11.3/IRDFF calculated ^{252}Cf spectrum averaged cross sections

Reaction	<RR>/<Φ>	<σ>	Reference Value	Reference	C/E	Trkov
^{24}Mg(n,p)	2.1332E−8 ± 0.071% / 1.0156E−5 ± 0.002%	2.100 mb ± 0.071 %	1.996 mb ± 2.4 %	Mannhart	1.052 ± 2.4%	1.055 ± 0.0302
^{32}S(n,p)	7.5155E−7 ± 0.015% / 1.0156E−5 ± 0.002%	74.00 mb ± 0.015 %	72.54 mb ± 3.5 %	Mannhart	1.020 ± 3.5%	1.0203 ± 0.0435
^{54}Fe(n,p)	8.7753E−7 ± 0.017% / 1.0156E−5 ± 0.002%	86.41 mb ± 0.017 %	86.84 mb ± 1.3 %	Mannhart	0.995 ± 1.3%	0.9955 ± 0.0343
^{56}Fe(n,p)	1.4833E−8 ± 0.055% / 1.0156E−5 ± 0.002%	1.461 mb ± 0.055 %	1.465 mb ± 1.8 %	Mannhart	0.997 ± 1.8%	0.9984 ± 0.0347
^{58}Ni(n,p)	1.1914E−6 ± 0.015% / 1.0156E−5 ± 0.002%	117.31 mb ± 0.015 %	117.50 mb ± 1.3 %	Mannhart	0.998 ± 1.3%	0.9984 ± 0.0229
^{59}Co(n,g)	4.9450E−8 ± 0.420% / 1.0156E−5 ± 0.002%	4.87 mb ± 0.42 %	6.97 mb ± 4.88 %	Csikai	**0.699** ± 4.9%	N/A
^{63}Cu(n,g)	1.0581E−7 ± 0.099% / 1.0156E−5 ± 0.002%	10.418 mb ± 0.099 %	10.3 mb ± 2.9 %	Manojlovič	1.012 ± 2.9%	1.0106 ± 0.0893
^{115}In(n,ng)	1.9342E−6 ± 0.008% / 1.0157E−5 ± 0.002%	190.4 mb ± 0.008 %	197.4 mb ± 1.4 %	Mannhart	0.965 ± 1.4%	0.966 ± 0.0218
^{115}In(n,g)	1.5564E−6 ± 0.008% / 1.0156E−5 ± 0.002%	153.25 mb ± 0.008 %	125.6 mb ± 2.1 %	Mannhart	**1.220** ± 2.1%	N/A
^{197}Au(n,g)	7.6210E−7 ± 0.037% / 1.0156E−5 ± 0.002%	75.04 mb ± 0.037 %	75.5 mb ± 1.3 %	Manojlovič	0.994 ± 1.3%	0.9931 ± 0.0185
^{232}Th(n,g)	9.1509E−7 ± 0.026% / 1.0156E−5 ± 0.002%	90.10 mb ± 0.026 %	87.0 mb ± 1.8 %	Manojlovič	1.036 ± 1.8%	1.0741 ± 0.0422
^{232}Th(n,f)	8.4640E−7 ± 0.010% / 1.0156E−5 ± 0.002%	83.34 mb ± 0.010 %	84.55 mb ± 2.3 %	Csikai	0.986 ± 2.3%	0.9864 ± 0.0820
^{235}U(n,f)	1.2458E−5 ± 0.002% / 1.0156E−5 ± 0.002%	1226.7 mb ± 0.002 %	1210.0 mb ± 1.2 %	Mannhart	1.014 ± 1.2%	1.0138 ± 0.0170
^{238}U(n,f)	3.2654E−6 ± 0.009% / 1.0157E−5 ± 0.002%	321.5 mb ± 0.009 %	325.7 mb ± 1.6 %	Mannhart	0.987 ± 1.6%	0.9872 ± 0.0209
^{237}Np(n,f)	1.3811E−5 ± 0.004% / 1.0156E−5 ± 0.002%	1359.9 mb ± 0.004 %	1361.0 mb ± 1.6 %	Mannhart	0.999 ± 1.6%	0.9991 ± 0.0233
^{239}Pu(n,f)	1.8259E−5 ± 0.002% / 1.0156E−5 ± 0.002%	1797.9 mb ± 0.003 %	1812.0 mb ± 1.4 %	Mannhart	0.992 ± 1.4%	0.9922 ± 0.0185

Notes: Values in **RED** correspond to $|C/E - 1| > 3\sigma$. IRDFF-II used for all calculations except IRDFF1.05 used for ^{115} In(n,ng). Trkov C/E values are for MCNP with IRDFF-II cross-sections except IRDFF1.02 used for ^{24}Mg(n,p) and ^{115}In(n,ng).

A. Trkov et al., "IRDFF-II: A New Neutron Metrology Library," Nuclear Data Sheets: 163 (2020) 1-108.

Cf-252 spectrum averaged cross sections.

Some problems observed with all libraries.

https://cog.llnl.gov

Table 2. Benchmark-Model and Calculated* Reaction Rate Ratios: COG11.3 with ENDF/B-VIII.0 used for particle transport and IRDFF-II for the reaction rate ratios (except IRDFF1.05 used for In115(n,ng))

Reaction Ratio	Benchmark-Model	Calculated	C/E
Th232(n,f)/U235(n,f)	0.043 ± 0.0013	(9.6130E-4 ± 1.1%)/(2.3149E-2 ± 0.7%) = 0.0415 ± 1.3%	0.966 ± 3.3%
U233(n,f)/U235(n,f)	1.54 ± 0.03	Not Available	
U234(n,f)/U235(n,f)	0.790 ± 0.024	Not Available	
U236(n,f)/U235(n,f)	0.333 ± 0.010	Not Available	
U238(n,f)/U235(n,f)	0.165 ± 0.005	(3.7648E-3 ± 1.0%)/(2.3149E-2 ± 0.7%) = 0.1626 ± 1.2%	0.986 ± 3.3%
Np237(n,f)/U235(n,f)	0.771 ± 0.023	(1.8992E-2 ± 1.4%)/(2.3149E-2 ± 0.7%) = 0.8204 ± 1.6%	1.064 ± 3.4%
Pu239(n,f)/U235(n,f)	1.33 ± 0.04	(3.1693E-2 ± 2.3%)/(2.3149E-2 ± 0.7%) = 1.3691 ± 2.4%	1.029 ± 3.9%
Pu240(n,f)/U235(n,f)	0.877 ± 0.026	Not Available	
Pu241(n,f)/U235(n,f)	1.29 ± 0.04	Not Available	
Pu242(n,f)/U235(n,f)	0.658 ± 0.020	Not Available	
Am241(n,f)/U235(n,f)	0.825 ± 0.025	(1.8179E-2 ± 0.8%)/(2.3149E-2 ± 0.7%) = 0.7853 ± 1.1%	0.952 ± 3.2%
Th232(n,g)/U235(n,f)	0.109 ± 0.004	(2.3382E-3 ± 0.8%)/(2.3149E-2 ± 0.7%) = 0.1010 ± 1.1%	0.927 ± 3.8%
U236(n,g)/U235(n,f)	0.123 ± 0.006	Not Available	
U238(n,g)/U235(n,f)	0.077 ± 0.003	(1.7699E-3 ± 1.0%)/(2.3149E-2 ± 0.7%) = 0.0765 ± 1.2%	0.993 ± 4.1%
Np237(n,g)/U235(n,f)	0.240 ± 0.012	Not Available	
Th232(n,2n)/U235(n,f)	0.00924 ± 0.00050	Not Available	
U238(n,2n)/U235(n,f)	0.00916 ± 0.00050	(2.3170E-4 ± 5.8%)/(2.3149E-2 ± 0.7%) = 0.0100 ± 5.8%	1.093 ± 8.0%
Nb93(n,2n)/U235(n,f)	0.000293 ± 0.000010	Not Available	
Al27(n,a)/U235(n,f)	0.00043 ± 0.00002	Not Available	
Fe54(n,a)/U235(n,f)	0.00050 ± 0.00002	Not Available	
Co59(n,a)/U235(n,f)	0.000095 ± 0.000004	Not Available	
Mo92(n,a)/U235(n,f)	0.000055 ± 0.000005	Not Available	
Nb93(n,a)/U235(n,f)	0.0000159 ± 0.0000009	Not Available	
Mg24(n,p)/U235(n,f)	0.00090 ± 0.00004	(2.2499E-5 ± 5.7%)/(2.3149E-2 ± 0.7%) = 0.00097 ± 5.7%	1.080 ± 7.3%
Al27(n,p)/U235(n,f)	0.00221 ± 0.00015	(4.7480E-5 ± 2.6%)/(2.3149E-2 ± 0.7%) = 0.00205 ± 2.7%	0.928 ± 7.3%
Ti46(n,p)/U235(n,f)	0.0066 ± 0.0003	(1.3836E-4 ± 2.8%)/(2.3149E-2 ± 0.7%) = 0.00598 ± 2.9%	0.906 ± 5.4%
Ti47(n,p)/U235(n,f)	0.0097 ± 0.0005	(2.1141E-4 ± 1.3%)/(2.3149E-2 ± 0.7%) = 0.00913 ± 1.5%	0.942 ± 5.4%
Ti48(n,p)/U235(n,f)	0.00018 ± 0.000008	(4.3657E-6 ± 5.5%)/(2.3149E-2 ± 0.7%) = 0.00019 ± 5.5%	1.048 ± 7.1%
Fe54(n,p)/U235(n,f)	0.0447 ± 0.0015	(8.9128E-4 ± 1.6%)/(2.3149E-2 ± 0.7%) = 0.03850 ± 1.7%	**0.861** ± 3.8%
Fe56(n,p)/U235(n,f)	0.00061 ± 0.00002	(1.4958E-5 ± 4.5%)/(2.3149E-2 ± 0.7%) = 0.00065 ± 4.6%	1.059 ± 5.6%
Ni58(n,p)/U235(n,f)	0.055 ± 0.003	(1.2317E-3 ± 1.4%)/(2.3149E-2 ± 0.7%) = 0.05321 ± 1.6%	0.967 ± 5.7%
Co59(n,p)/U235(n,f)	0.00084 ± 0.00004	(1.7127E-5 ± 2.7%)/(2.3149E-2 ± 0.7%) = 0.00074 ± 2.8%	0.881 ± 5.5%
Mo92(n,p)/U235(n,f)	0.00388 ± 0.00015	Not Available	
Cr50(n,g)/U235(n,f)	0.0557 ± 0.0005	Not Available	
Mn55(n,g)/U235(n,f)	0.00297 ± 0.00015	(8.6878E-5 ± 2.9%)/(2.3149E-2 ± 0.7%) = 0.00375 ± 3.0%	**1.264** ± 5.9%
Fe58(n,g)/U235(n,f)	0.00228 ± 0.00009	(5.5704E-5 ± 4.6%)/(2.3149E-2 ± 0.7%) = 0.00241 ± 4.7%	1.055 ± 6.1%
Co59(n,g)/U235(n,f)	0.0064 ± 0.0003	(1.3755E-4 ± 3.7%)/(2.3149E-2 ± 0.7%) = 0.00594 ± 3.8%	0.928 ± 6.0%
Ni64(n,g)/U235(n,f)	0.00185 ± 0.00008	Not Available	
Cu63(n,g)/U235(n,f)	0.0114 ± 0.0005	(2.7693E-4 ± 2.0%)/(2.3149E-2 ± 0.7%) = 0.01196 ± 2.1%	1.049 ± 4.9%
Cu65(n,g)/U235(n,f)	0.0076 ± 0.0006	Not Available	
Mo98(n,g)/U235(n,f)	0.0193 ± 0.0008	Not Available	
Zr94(n,g)/U235(n,f)	0.0064 ± 0.0004	Not Available	
Zr96(n,g)/U235(n,f)	0.00306 ± 0.006	Not Available	
Au197(n,g)/U235(n,f)	0.105 ± 0.005	(2.2966E-3 ± 1.1%)/(2.3149E-2 ± 0.7%) = 0.09921 ± 1.3%	0.945 ± 4.9%
In115(n,ng)/U235(n,f)	0.102 ± 0.006	(2.3029E-3 ± 0.9%)/(2.3149E-2 ± 0.7%) = 0.99482 ± 1.1%	0.975 ± 6.0%

*Calculated at midplane of Pu rods in a radius of 0.46 cm and height of 1 cm. Files: BR1-0 and BR1-1. Results in **RED** have |C/E-1|>3σ.

FUND-IPPE-FR-MULT-RRR-001

BR-1 reactor spectral indices

https://cog.llnl.gov

Conclusion: The following COG11.3 cross-section libraries produce calculated results consistent with BR-1 benchmark values.

Table 4. Recommended Libraries for Reaction Rate Calculations

Th232(n,f)	IRDFF-II ENDFB8R0
U233(n,f)	JEFF3.3 ENDFB8R0
U234(n,f)	JEFF3.3* ENDFB8R0*
U236(n,f)	ENDFB8R0
U238(n,f)	IRDFF-II ENDFB8R0
Np237(n,f)	ENDFB8R0 IRDFF-II
Pu239(n,f)	ENDFB8R0 IRDFF-II
Pu240(n,f)	JEFF3.3 ENDFB8R0
Pu241(n,f)	ENDFB8R0
Pu242(n,f)	ENDFB8R0
Am241(n,f)	JEFF3.3 IRDFF-II ENDFB8R0

Th232(n,g)	JEFF3.3 ENDFB8R0 IRDFF-II
U236(n,g)	ENDFB8R0
U238(n,g)	IRDFF-II ENDFB8R0
Np237(n,g)	None

Th232(n,2n)	ENDFB8R0
U238(n,2n)	JEFF3.3 ENDFB8R0
Nb93(n,2n)	None

Al27(n,a)	JEFF3.3 ENDFB8R0
Fe54(n,a)	ENDFB8R0
Co59(n,a)	JEFF3.3 ENDFB8R0
Mo92(n,a)	JEFF3.3
Nb93(n,a)	None

Mg24(n,p)	IRDFF-II
Al27(n,p)	ENDFB8R0 IRDFF-II
Ti46(n,p)	IRDFF-II
Ti47(n,p)	IRDFF-II
Ti48(n,p)	IRDFF-II
Fe54(n,p)	ENDFB8R0
Fe56(n,p)	IRDFF-II ENDFB8R0
Ni58(n,p)	IRDFF-II
Co59(n,p)	IRDFF-II JEFF3.3
Mo92(n,p)	IRDFF-II

Cr50(n,g)	None
Mn55(n,g)	None
Fe58(n,g)	IRDFF-II JEFF3.3
Co59(n,g)	IRDFF-II
Ni64(n,g)	None
Cu63(n,g)	ENDFB8R0 IRDFF-II
Cu65(n,g)	JEFF3.3 ENDFB8R0
Mo98(n,g)	JEFF3.3
Zr94(n,g)	JEFF3.3
Zr96(n,g)	None
Au197(n,g)	ENDFB8R0 IRDFF-II JEFF3.3

In115(n,ng)	IRDFF1.05

* In these cases, $|C/E-1| > 3\sigma$ (slightly).

FUND-IPPE-FR-MULT-RRR-001

BR-1 reactor spectral indices are useful for nuclear data selection

https://cog.llnl.gov

COG 11.3 Results Using ENDF/B-VIII.0 for Transport and IRDFF-II for Reaction Rates

Table B-1. Godiva (HMF001)

Spectral Index	COG11.3 Calculation	Experiment	Ref.	C/E
Mn55(n,g)/U235(n,f)	$\frac{(5.5971\text{-}5 \pm 0.74\%)}{(1.6448\text{-}2 \pm 0.25\%)} = 0.0034 \pm 0.78\%$	$0.0027 \pm 7.41\%$	Trkov Pelloni	**1.26** $\pm$ 7.45%
Co59(n,g)/U235(n,f)	$\frac{(1.0267\text{-}4 \pm 0.53\%)}{(1.6448\text{-}2 \pm 0.25\%)} = 0.0062 \pm 0.59\%$	$0.0380 \pm 7.89\%$	Trkov Pelloni	**0.16** $\pm$ 7.91%
Cu63(n,g)/U235(n,f)	$\frac{(1.8740\text{-}4 \pm 0.55\%)}{(1.6448\text{-}2 \pm 0.25\%)} = 0.0114 \pm 0.60\%$	$0.0117 \pm 5.13\%$	Trkov Pelloni	$0.97 \pm 5.17\%$
Nb93(n,g)/U235(n,f)	$\frac{(5.2523\text{-}4 \pm 0.50\%)}{(1.6448\text{-}2 \pm 0.25\%)} = 0.0319 \pm 0.56\%$	$0.0300 \pm 10.0\%$	Trkov Pelloni	$1.06 \pm 10.0\%$
La139(n,g)/U235(n,f)	$\frac{(1.0459\text{-}4 \pm 0.39\%)}{(1.6448\text{-}2 \pm 0.25\%)} = 0.0064 \pm 0.46\%$	$0.0073 \pm 8.22\%$	Trkov	$0.87 \pm 8.23\%$
Ta181(n,g)/U235(n,f)	$\frac{(1.6772\text{-}3 \pm 0.44\%)}{(1.6448\text{-}2 \pm 0.25\%)} = 0.1020 \pm 0.51\%$	$0.1230 \pm 9.76\%$	Trkov	$0.83 \pm 9.77\%$
Au197(n,g)/U235(n,f)	$\frac{(1.5583\text{-}3 \pm 0.34\%)}{(1.6448\text{-}2 \pm 0.25\%)} = 0.0947 \pm 0.42\%$	$0.1000 \pm 2.00\%$	Trkov Pelloni	$0.95 \pm 2.04\%$
U233(n,f)/U235(n,f)	U233(n,f) not available in IRDFF-II	1.59 $\pm$ 1.89%	Alwin Pelloni	N/A
U238(n,f)/U235(n,f)	$\frac{(2.5764\text{-}3 \pm 0.39\%)}{(1.6448\text{-}2 \pm 0.25\%)} = 0.1566 \pm 0.46\%$	$0.1643 \pm 1.10\%$ $0.1647 \pm 1.09\%$	Alwin Pelloni	**0.95** $\pm$ 1.19% **0.95** $\pm$ 1.18%
Np237(n,f)/U235(n,f)	$\frac{(1.3685\text{-}2 \pm 0.29\%)}{(1.6448\text{-}2 \pm 0.25\%)} = 0.8320 \pm 0.38\%$	$0.8516 \pm 1.41\%$ $0.837 \pm 1.55\%$	Alwin Pelloni	$0.98 \pm 1.46\%$ $0.99 \pm 1.60\%$
Pu239(n,f)/U235(n,f)	$\frac{(2.2765\text{-}2 \pm 0.24\%)}{(1.6448\text{-}2 \pm 0.25\%)} = 1.3841 \pm 0.35\%$	$1.4152 \pm 0.99\%$ $1.402 \pm 1.78\%$	Alwin Pelloni	$0.98 \pm 1.05\%$ $0.99 \pm 1.81\%$
Al27(n,a)/P31(n,p)	Al27(n,a) not available in IRDFF-II	$0.0215 \pm 3.55\%$	Trkov	N/A
Al27(n,p)/P31(n,p)	$\frac{(3.1300\text{-}5 \pm 1.02\%)}{(2.7897\text{-}4 \pm 0.51\%)} = 0.1122 \pm 1.14\%$	$0.1126 \pm 4.88\%$	Trkov	$1.00 \pm 5.01\%$
Fe56(n,p)/P31(n,p)	$\frac{(8.7986\text{-}6 \pm 1.88\%)}{(2.7897\text{-}4 \pm 0.51\%)} = 0.0315 \pm 1.95\%$	$0.0310 \pm 5.80\%$	Trkov	$1.02 \pm 6.12\%$

File: HMF001-1-SI-0.

Spectral indices for 9 LANL fast critical assemblies:

- Godiva
- Flattop-25
- Big-Ten
- Jezebel
- Flattop-Pu
- Thor
- Jezebel-23
- Flattop-23
- Dirty Jezebel

https://cog.llnl.gov

Work in progress – ICSBEP k-eff benchmark intercomparison project in progress

	A
1	LLNL-MI-838253
2	
3	COG Benchmark Results (3395)
4	
5	David P. Heinrichs
6	Soon S. Kim
7	
8	
9	
10	28-Jul-22
11	
12	
13	
14	Nuclear Criticality Safety Division
15	Lawrence Livermore National Laboratory
16	7000 East Avenue, L-198, Livermore, CA, 94550, USA
17	
18	
19	This work was performed under the auspices of the U.S. Department of Energy by Lawrence Livermore National Laboratory under Contract DE-AC52-07NA27344.
20	

Spreadsheet with 3,395 ICSBEP benchmark k-eff's

- ENDF/B-VII.1
- ENDF/B-VIII.0
- JEFF-3.3

Code intercomparison with COG, MCNP, MORET, SCALE (and MERCURY)

https://cog.llnl.gov

Work in progress – Subcritical benchmarks too!

Implemented FREYA in COG to improve R2F simulation of the ISSA. Much higher additional subcritical multiplication experiments by IRSN, LANL and LLNL are in progress at SNL using 7uPCX.

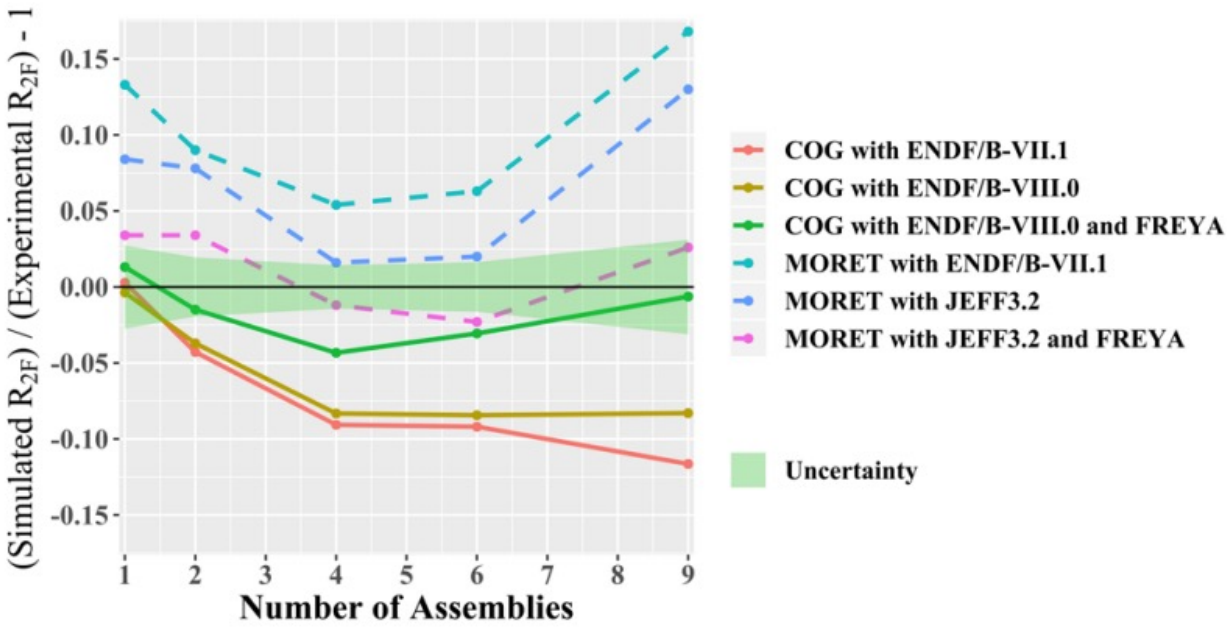

Figure 7. Difference between simulated and experimental R_{2F} values for each configuration.

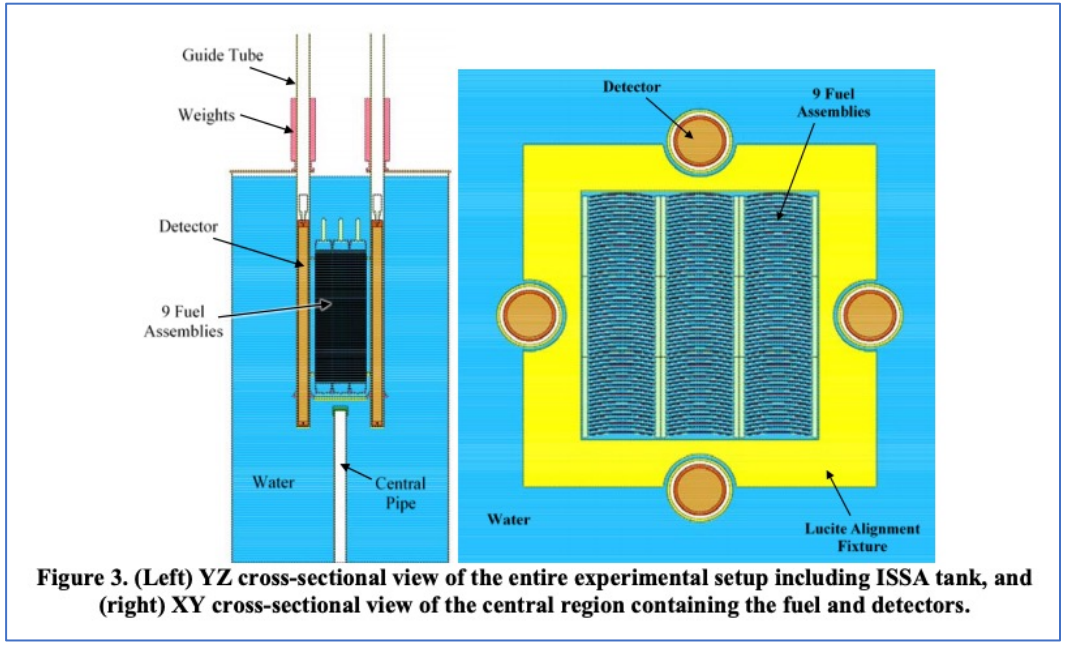

Figure 3. (Left) YZ cross-sectional view of the entire experimental setup including ISSA tank, and (right) XY cross-sectional view of the central region containing the fuel and detectors.

A. Nelson et al., "Fundamental Physics Subcritical Neutron Multiplicity Benchmark Experiments Using Water Moderated Highly Enriched Uranium Fuel" – ICNC 2019

Work in progress – Ueki single slab and multi-slab shield benchmarks

Many excellent benchmarks have yet to be evaluated and published in international compendia like ICSBEP and SINBAD. One much used example is:

NSE: **124**, 455-464 (1996), Systematic Evaluation of Neutron Shielding Effects for Materials, K. Ueki et al.

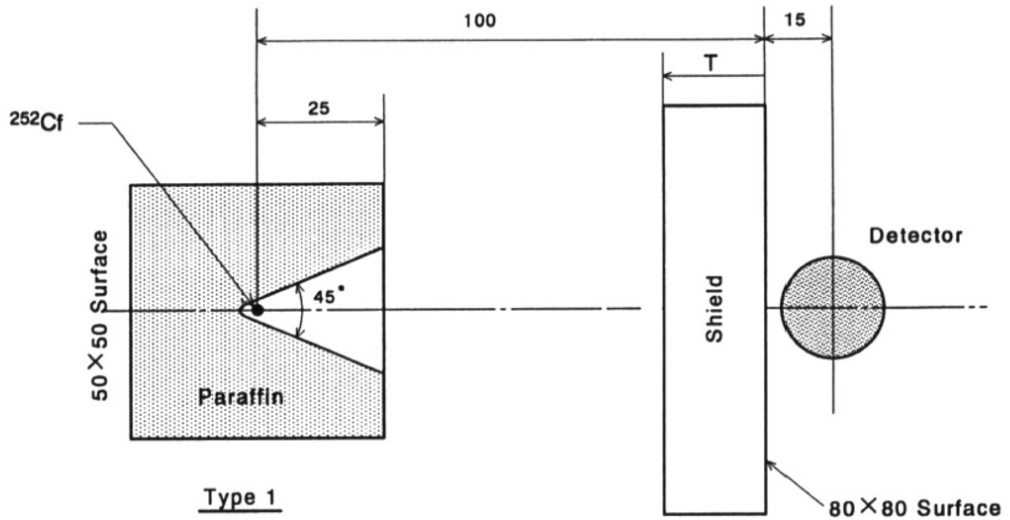

Table 1A – Type 1 Polyethylene Slab Shields (1.9620×10^{15} μn•Sv/hr•REM)

Shield	Experiment[1] (μSv/hr, ± 15%)	Cf-252 Source	COG (REM/n)	COG (μSv/hr)	C/E	File
None	683	Watt	(311.7 ± 0.7) E-15	611.6 ± 1.4	0.90 ± 15%	ueki-w-t1-0
5 cm CH2	288	Watt	(147.6 ± 1.2) E-15	289.6 ± 2.4	1.01 ± 15%	ueki-w-t1-p5
10 cm CH2	110	Watt	(600.0 ± 8.0) E-16	117.7 ± 1.6	1.07 ± 15%	ueki-w-t1-p10
15 cm CH2	42.6	Watt	(263.8 ± 5.8) E-16	51.8 ± 1.1	1.22 ± 15%	ueki-w-t1-p15
20 cm CH2	18.3	Watt	(110.8 ± 3.3) E-16	21.7 ± 0.6	1.19 ± 15%	ueki-w-t1-p20
25 cm CH2	8.3	Watt	(477.8 ± 7.1) E-17	9.37 ± 0.14	1.14 ± 15%	ueki-w-t1-p25
30 cm CH2	3.5	Watt	(223.0 ± 4.9) E-17	4.38 ± 0.10	1.25 ± 15%	ueki-w-t1-p30
None	683	IRDFF	(311.1 ± 0.8) E-15	610.4 ± 1.6	0.89 ± 15%	ueki-t-t1-0
5 cm CH2	288	IRDFF	(145.4 ± 1.2) E-15	285.3 ± 2.4	0.98 ± 15%	ueki-t-t1-p5
10 cm CH2	110	IRDFF	(595.4 ± 7.8) E-16	116.8 ± 1.5	1.06 ± 15%	ueki-t-t1-p10
15 cm CH2	42.6	IRDFF	(249.3 ± 5.4) E-16	48.9 ± 1.1	1.15 ± 15%	ueki-t-t1-p15
20 cm CH2	18.3	IRDFF	(109.5 ± 3.6) E-16	21.5 ± 0.7	1.17 ± 15%	ueki-t-t1-p20
25 cm CH2	8.3	IRDFF	(475.5 ± 7.4) E-17	9.33 ± 0.15	1.12 ± 15%	ueki-t-t1-p25
30 cm CH2	3.5	IRDFF	(219.6 ± 4.9) E-17	4.31 ± 0.10	1.23 ± 15%	ueki-t-t1-p30
None	683	FREYA	(318.6 ± 0.7) E-15	625.1 ± 1.4	0.92 ± 15%	ueki-f-t1-0
5 cm CH2	288	FREYA	(158.3 ± 3.6) E-15	310.6 ± 7.1	1.08 ± 15%	ueki-f-t1-p5
10 cm CH2	110	FREYA	(697.7 ± 8.9) E-16	136.9 ± 1.7	1.24 ± 15%	ueki-f-t1-p10
15 cm CH2	42.6	FREYA	(306.7 ± 6.1) E-16	60.2 ± 1.2	1.41 ± 15%	ueki-f-t1-p15
20 cm CH2	18.3	FREYA	(146.7 ± 4.1) E-16	28.8 ± 0.8	1.57 ± 15%	ueki-f-t1-p20
25 cm CH2	8.3	FREYA	(684.4 ± 8.8) E-17	13.4 ± 0.17	1.62 ± 15%	ueki-f-t1-p25
30 cm CH2	3.5	FREYA	(381.1 ± 7.5) E-17	7.48 ± 0.15	2.14 ± 15%	ueki-f-t1-p30

Work in progress – SINBAD Winfrith Water Benchmark

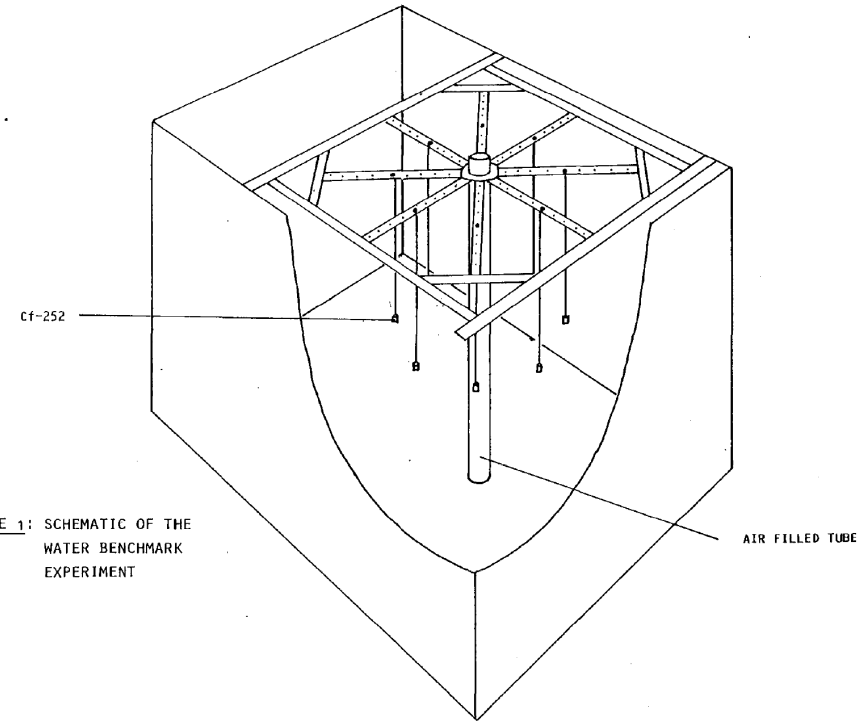

FIGURE 1: SCHEMATIC OF THE WATER BENCHMARK EXPERIMENT

Winfrith Water Benchmark

COG 11.3 Results: S32(n,pg)P32 reaction rates

File	Horizontal Separation (cm)	Axial Displacement (cm)	Calculated Reaction Rate (dps/nps•cc)	Calculated* Reaction Rate (dps/atom•nps)	Measured** Reaction Rate (dps/atom•nps)	C/E*
winfrith-10-0	10.16	0	1.021E-6 ± 0.1%	3.077E-29 ± 0.1%	3.19E-29 ± 6%	0.96 ± 6%
winfrith-10-15	10.16	15	1.791E-7 ± 0.2%	5.396E-30 ± 0.2%	5.37E-30 ± 6%	1.00 ± 6%
winfrith-10-30	10.16	30	2.171E-8 ± 0.7%	6.541E-31 ± 4.2%	6.71E-31 ± 6%	0.97 ± 6%
winfrith-15-0	15.24	0	2.559E-7 ± 0.2%	7.710E-30 ± 0.2%	7.56E-30 ± 6%	1.02 ± 6%
winfrith-15-15	15.24	15	7.544E-8 ± 0.4%	2.273E-30 ± 0.4%	2.25E-30 ± 6%	1.01 ± 6%
winfrith-15-30	15.24	30	1.099E-8 ± 1.0%	3.310E-31 ± 1.0%	3.22E-31 ± 6%	1.03 ± 6%
winfrith-25-0	25.40	0	2.886E-8 ± 0.6%	8.695E-31 ± 0.6%	8.55E-31 ± 6%	1.02 ± 6%
winfrith-25-15	25.40	15	1.438E-8 ± 0.9%	4.332E-31 ± 0.9%	4.36E-31 ± 6%	0.99 ± 6%
winfrith-25-30	25.40	30	3.163E-9 ± 1.9%	9.530E-32 ± 1.9%	9.50E-32 ± 6%	1.00 ± 6%
winfrith-30-0	30.45	0	1.146E-8 ± 1.0%	3.452E-31 ± 1.0%	3.43E-31 ± 6%	1.01 ± 6%
winfrith-30-15	30.45	15	6.497E-9 ± 1.3%	1.957E-31 ± 1.3%	1.94E-31 ± 6%	1.01 ± 6%
winfrith-30-30	30.45	30	1.706E-9 ± 2.7%	5.141E-32 ± 2.7%	5.16E-32 ± 6%	1.00 ± 7%
winfrith-35-0	35.56	0	4.759E-9 ± 1.6%	1.434E-31 ± 1.6%	1.42E-31 ± 6%	1.01 ± 6%
winfrith-35-15	35.56	15	2.926E-9 ± 2.0%	8.815E-32 ± 1.6%	8.92E-32 ± 6%	0.99 ± 6%
winfrith-35-30	35.56	30	9.514E-10 ± 3.6%	2.866E-32 ± 3.6%	2.81E-32 ± 6%	1.02 ± 7%

*1E+9 neutrons. To convert from dps/nps•cc to dps/atom•nps multiply by (17.24106 cc) and divide by (5.72275E+23 atoms).
**The uncertainty in the S32(n,pg)P32 saturated dps/atom measured values is ±6%.

Work in progress – ALARM-CF-AIR-LAB-001

ALARM-CF-AIR-LAB-001
Neutron Fields in Three-Section Concrete Labyrinth from Cf-252 Source
Experiments performed in 1982 at the Institute of High Energy Physics at Protvino,

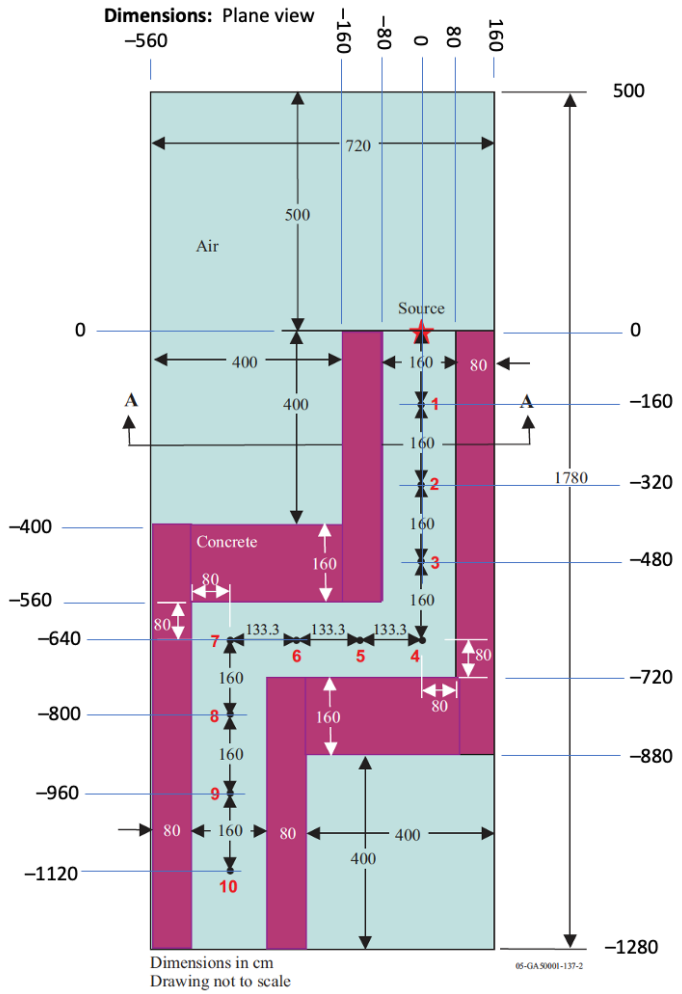

Figure 13. View of the Labyrinth in Horizontal Cross Section, Case 1.

ALARM-CF-AIR-LAB-001

Dimensions: Axial view of the detector

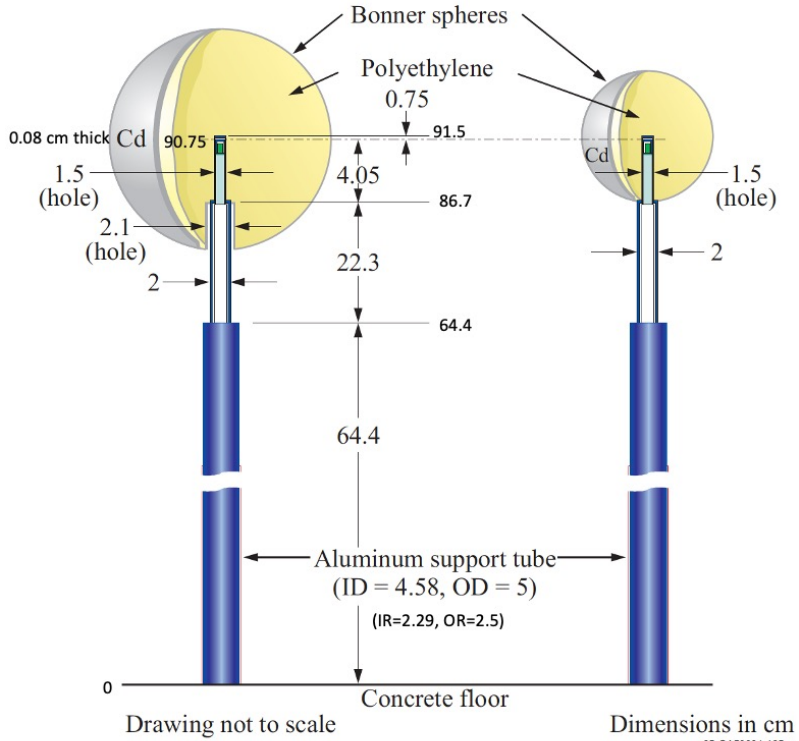

Figure 20. Model of Detector.

Lo-Fi results using evaluators' detector response function:

Table 1. Case 1A with 2" Bonner Sphere

Position	Calculation*	Experiment**	C/E
1	1524 ± 5%	1320 ± 8%	1.15 ± 9%
2	634 ± 7%	617 ± 10%	1.03 ± 12%
3	273 ± 3%	284 ± 11%	0.96 ± 11%
4	156 ± 7%	155 ± 11%	1.01 ± 13%
5	66.6 ± 7%	70.7 ± 13%	0.94 ± 15%
6	29.3 ± 11%	25.7 ± 14%	1.14 ± 18%
7	11.8 ± 6%	13.0 ± 14%	0.91 ± 15%
8	3.37 ± 11%	4.16 ± 17%	0.81 ± 20%
9	0.937 ± 7%	1.25 ± 18%	0.75 ± 19%
10	0.661 ± 37%	0.605 ± 19%	1.09 ± 42%

*Li6(n,tg) reactions/sec. **Detector pulses/sec. File: protvino1a-2-0

Hi-Fi calculation with Bonner sphere explicitly modeled in progress. The far field will require 1E+12 neutron histories (or more)

Work in progress – ALARM-REAC-AIR-SKY-001 – Baikal-1 Skyshine Benchmark

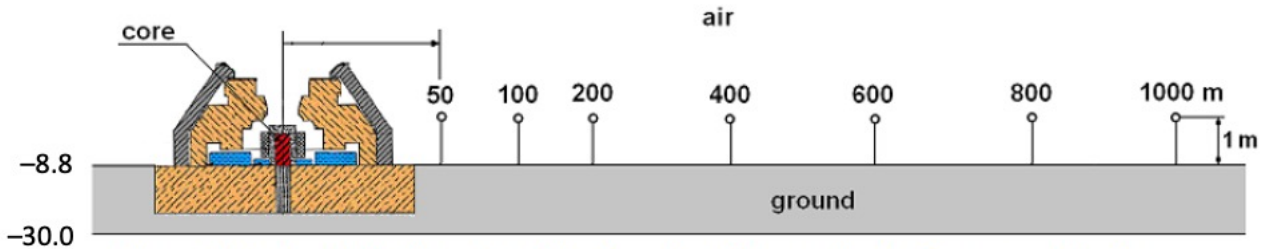

Figure 1.1. Schematic Configuration of the Experiment Showing On-site Measurement Positions. (not to scale)

ALARM-REAC-AIR-SKY-001

Benchmark-Model and Sample Results: Baikal-1 (case 1) neutron dose rates

Distance meter	ρR g/cm²	COG REM/(fission/sec)	COG μSv/hr	Experiment* μSv/hr	C/E
13 November 1996 with ρ(air) = 1.364E-3 g/cc.					
50	6.82	1.043E-18 ± 1.2%	3.33E+5	3.22E+5	1.03 ± 19%
100	13.64	3.107E-19 ± 1.7%	9.91E+4	9.90E+4	1.00 ± 19%
200	27.28	6.392E-20 ± 2.6%	2.04E+4	1.80E+4	1.13 ± 19%
300	40.92	1.886E-20 ± 5.2%	6.02E+3	4.53E+3	1.33 ± 20%
400	54.56	5.319E-21 ± 7.1%	1.70E+3	1.64E+3	1.03 ± 20%
500	68.20	2.068E-21 ± 11.1%	6.60E+2	5.13E+2	1.29 ± 22%
600	81.84	6.463E-22 ± 15.4%	2.06E+2	1.73E+2	1.19 ± 24%
800	109.12	1.603E-22 ± 26.3%	5.12E+1	2.60E+1	1.97 ± 32%
1000	136.40	2.529E-23 ± 68.2%	8.07E+0	4.64E+0	1.74 ± 71%

*Experimental results are ±19%. File: Baikal-1

(1 Rem per fission/sec)(8.886367E+15 fissions/sec per 300 kW)(60 sec/min)(60 min/hr)(1E+6 μSv/Sv)(1 Sv/100 Rem) =3.191E+23 μSv/hr.

Lo-Fi neutron dose results shown.

Delayed fission gamma problem in COG 11.3 (waiting for bug fix)

Work in progress – LLNL Pulsed Spheres – External review in progress by SINBAD TRG

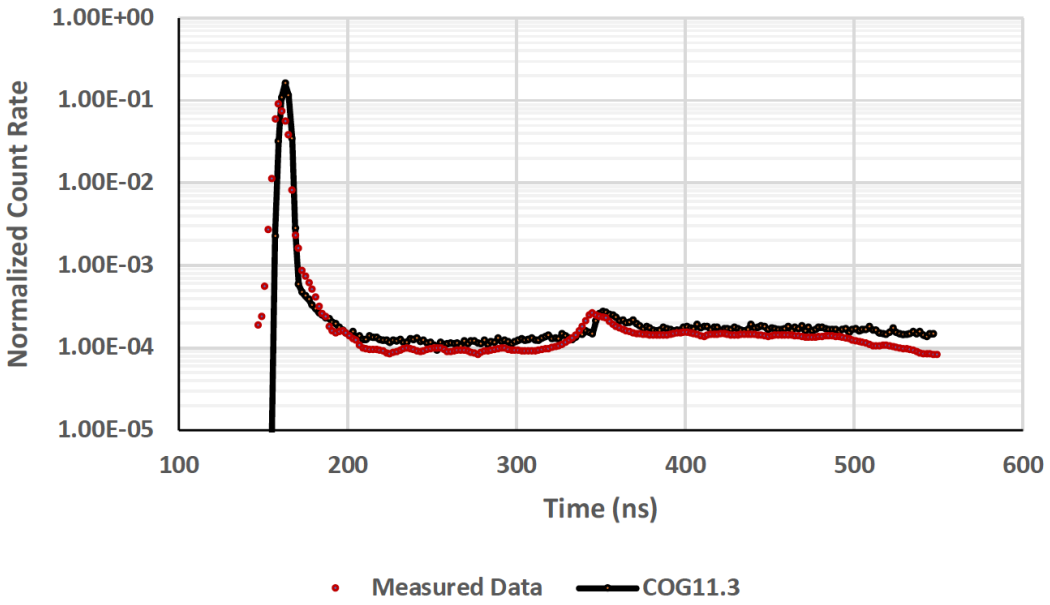

Figure 21. Normalized Count Rate vs. Time for the Blank Case.

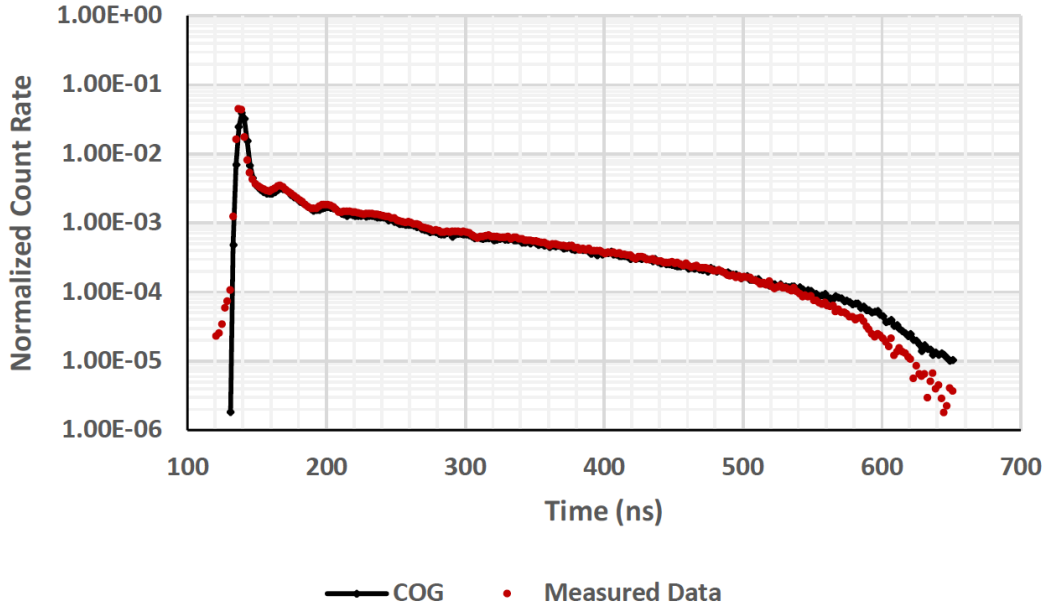

Figure 22. Normalized Count Rate vs. Time for the Polyethylene Case.

Work in progress – Godiva-IV PDV dynamic benchmark

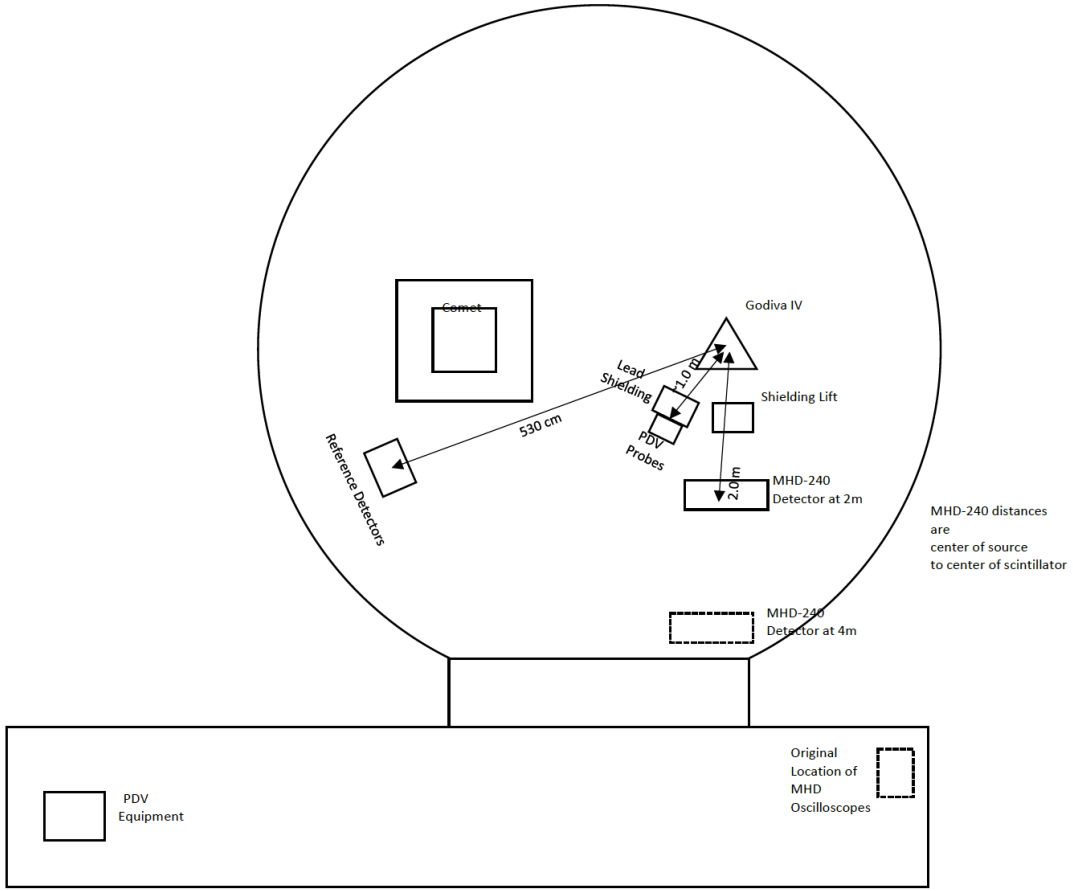

Equipment Setup Diagram for IER 268

(LA-UR-21-21533)

(LLNL-TR-826595)

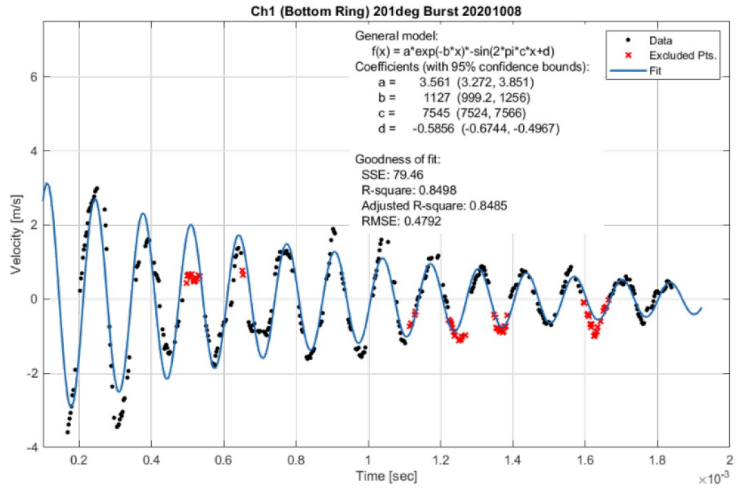

Figure 4: PDV data collected on the bottom ring of Godiva during the 201°C burst. Data points are extracted from the raw data and then fit to determine the vibration frequency. The fit function and various fit parameters are listed in the legend.

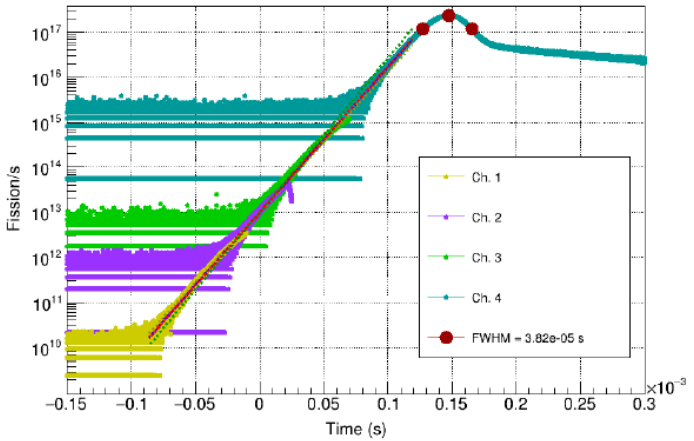

Figure 7: MHD-240 data for the 201°C burst as measured by the 4 channels of the MHD-240. The vertical axis is scaled based on the gamma calibration. The neutron calibration was not considered in this plot. The dashed lines shown are the exponential fit results to each of the channels data.

Work in progress – Neutron spectra measurements with a portable instrument

- Initially developed in 2013.
- Used for a test measurement of the GODIVA sub-critical assembly.
- Un-reduceable correlated backgrounds resulted in inaccuracies in the result.

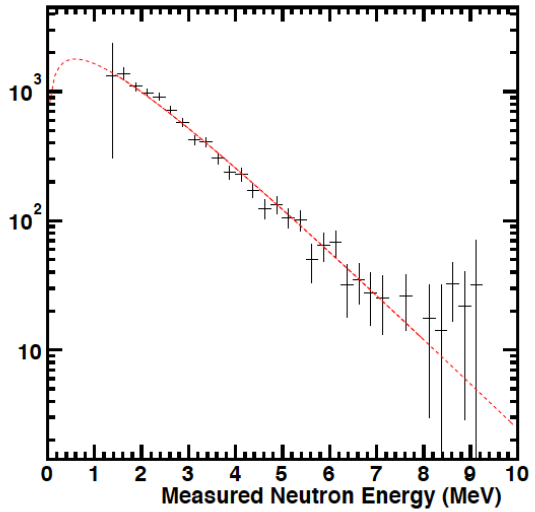

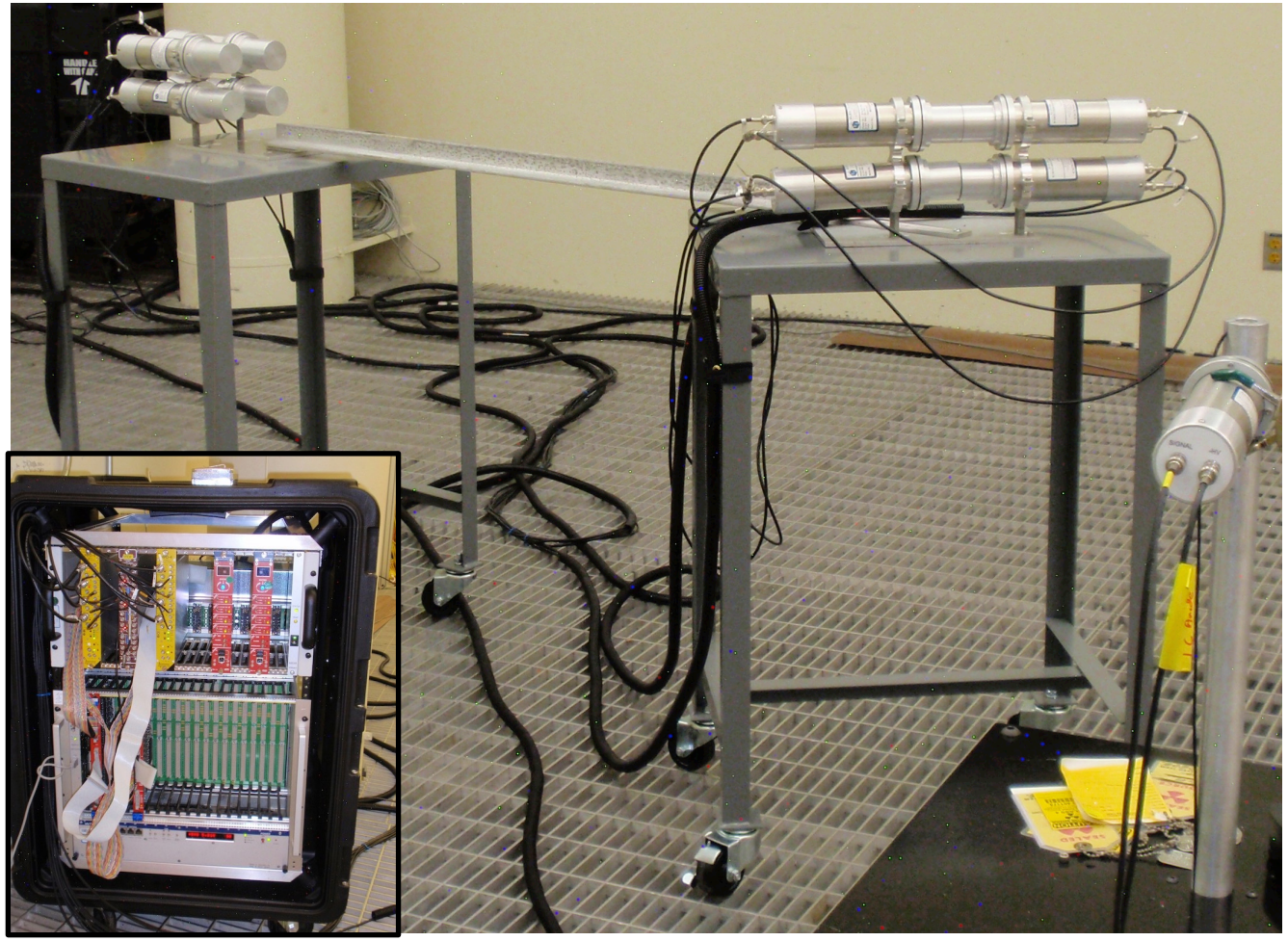

Work in progress – Neutron spectra measurement calibration at Ohio University

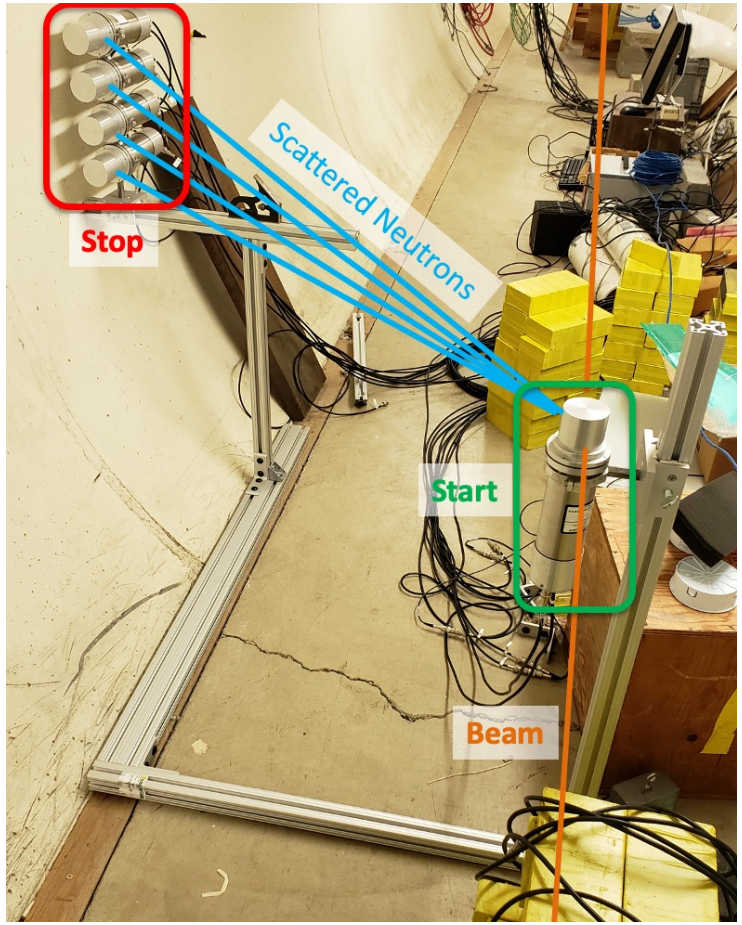

- Energy spectra from the hNTOF(blue) compared to the reference data (black) from Ohio University.
- Low efficiency due to the double scatter requirement
- Good energy resolution between 2 and 11 MeV incident neutron energy

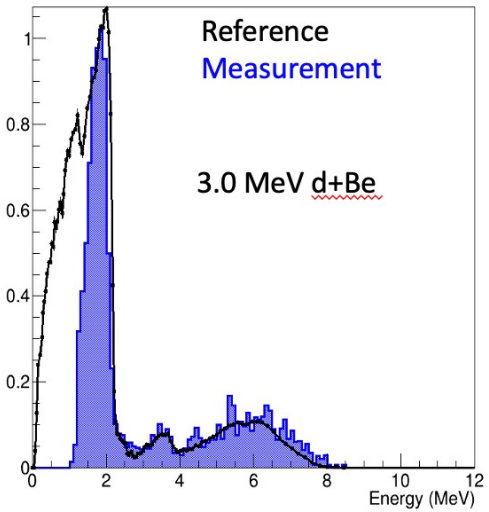

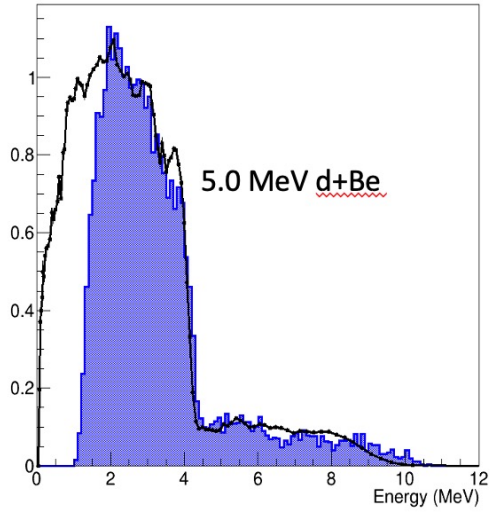

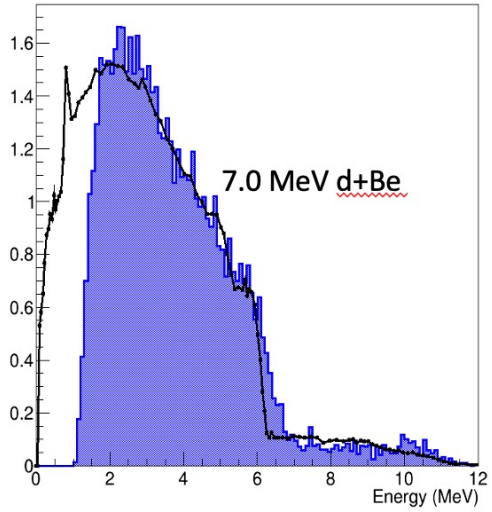

Work in progress – Neutron spectra measurements of AmBe in a low scatter LLNL facility

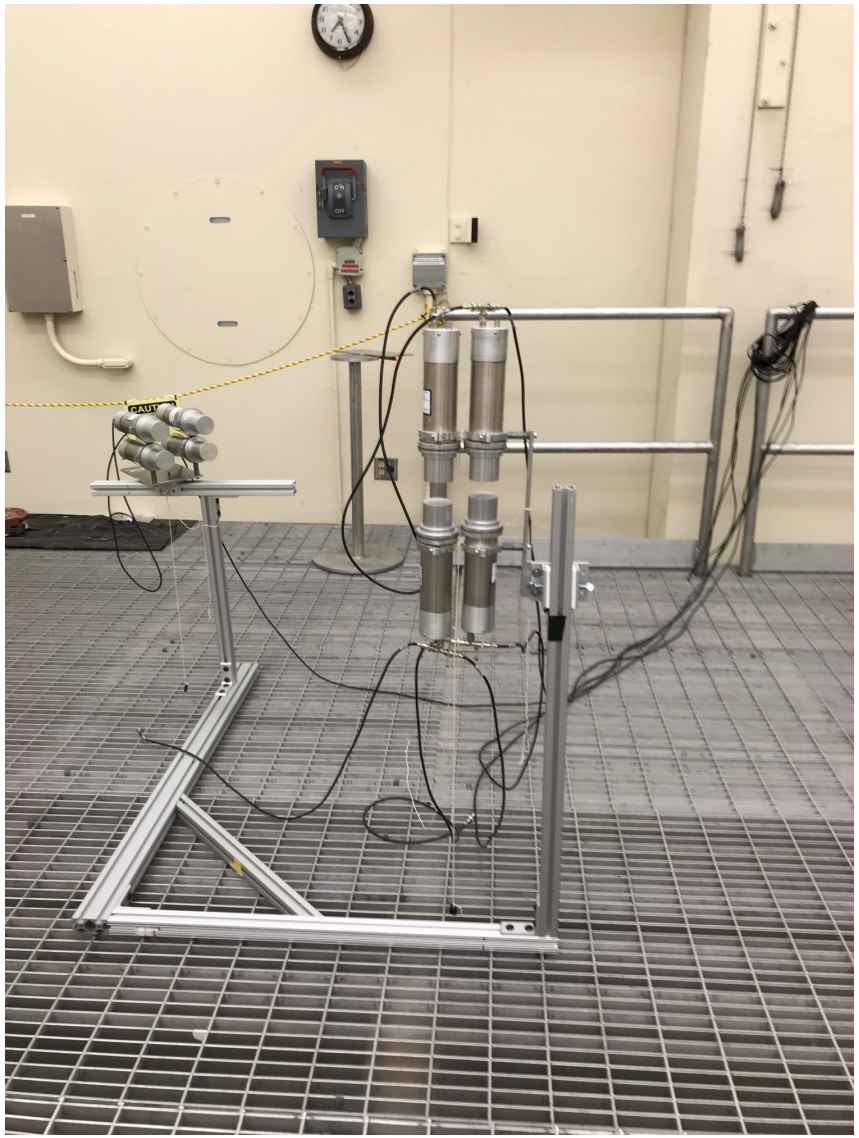

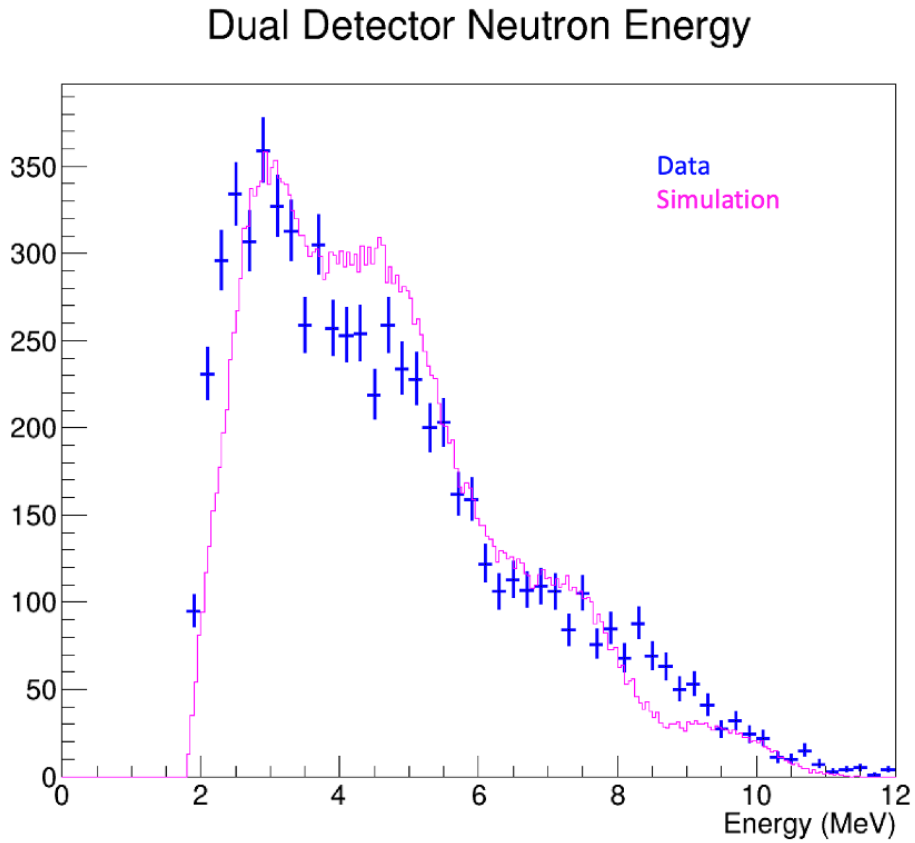

Simulation improvements to include source capsule construction and room details.

Doubling the number of detectors to quadruple efficiency.

Work in progress – Delayed critical $\alpha_{DC} = -\beta/\ell = 1/\Lambda - 1/\ell$

Table I. Comparison of calculated and measured values for selected kinetics parameters in critical systems. Calculated results were generated using track-length estimators in the MC21 Monte Carlo code.

Core	Calculated				Measured		C/E	
	k_{eff} (95% CI)	β_{eff} [pcm] (1σ)	Λ_{eff} [μs] (1σ)	-α [$\times 10^4$/sec] (1σ)	β_{eff} [pcm] (1σ)	-α [$\times 10^4$/sec] (1σ)	β_{eff}	α
Godiva	0.9999(2)	642(1)	0.00572(1)	112.6(4)	659(10)	111(2)	0.97	1.01
Jezebel	0.9998(2)	184(7)	0.002874(9)	64.4(3)	194(10)	64(1)	0.95	1.01
Jezebel-U233	0.9996(2)	293(1)	0.002736(9)	107.4(5)	290(10)	100(1)	1.01	1.07
Flattop-Pu	1.0001(2)	258(1)	0.01321(8)	19.9(1)	276(7)	21.4(5)	0.93	0.93
Flattop-U235	1.0029(2)	622(1)	0.01742(8)	36.1(2)	665(13)	38.2(2)	0.94	0.95
Flattop-U233	0.9994(2)	336(1)	0.01264(8)	27.1(2)	360(9)	26.7(5)	0.93	1.01
Big Ten	1.0046(2)	698(1)	0.0604(1)	11.60(6)	720(37)	11.7(1)	0.97	0.99
Zeus-1	0.9931(3)	730(3)	1.99(2)	0.40(2)	--	0.338(8)	--	1.18
Zeus-2	0.9970(3)	735(2)	1.04(1)	0.75(1)	--	0.61(6)	--	1.23
Zeus-3	1.0008(3)	732(2)	0.521(4)	1.45(5)	--	1.19(1)	--	1.22
Zeus-4	1.0071(3)	728(2)	0.222(2)	3.41(4)	--	2.62(2)	--	1.30
STACY-28	1.0013(1)	727(1)	56.20(7)	0.01294(2)	--	0.0131(4)	--	0.99
STACY-29	1.0014(2)	719(1)	59.5(1)	0.01210(3)	--	0.0123(4)	--	0.98
STACY-30	0.9970(2)	729(1)	58.5(1)	0.01248(4)	--	0.0127(3)	--	0.98
STACY-33	0.9994(2)	715(1)	62.7(1)	0.01142(3)	--	0.0117(4)	--	0.98
STACY-35	1.0016(1)	711(1)	65.01(6)	0.01093(2)	--	0.0110(6)	--	0.99
STACY-46	1.0017(2)	703(1)	67.1(1)	0.01047(3)	--	0.0106(4)	--	0.99
STACY-52	1.0005(1)	703(1)	68.85(6)	0.01023(1)	--	0.0104(4)	--	0.98
STACY-55	1.0007(1)	700(1)	70.29(6)	0.01000(1)	--	0.0102(3)	--	0.98
STACY-118	1.0042(1)	747(1)	43.72(5)	0.01711(3)	--	0.0169(3)	--	1.01
STACY-125	1.0044(2)	737(1)	48.82(9)	0.01513(4)	--	0.0153(3)	--	0.99
STACY-128	1.0028(1)	733(1)	51.00(6)	0.01438(2)	--	0.0145(3)	--	0.99

… and many more (FCA, TCA, SHE)

Work in progress – Pulse Neutron Die-Away (–α) in Moderators w/w/o Absorbers

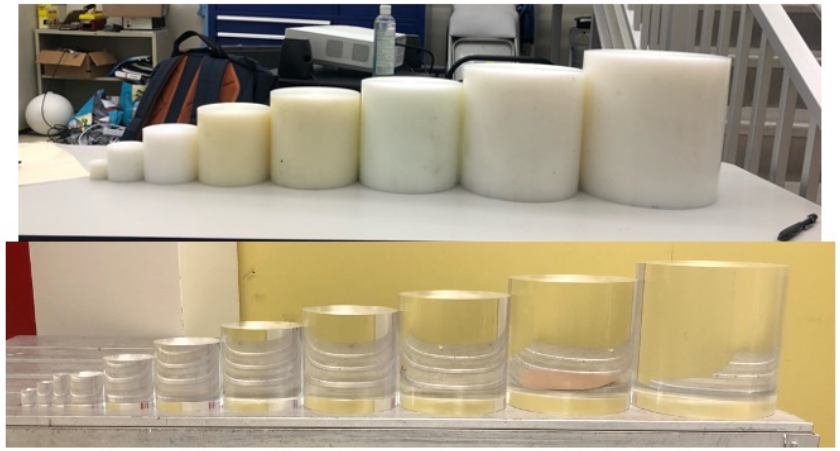

Figure 2.5: Some of the HDPE (top) and Lucite (bottom) cylinders.

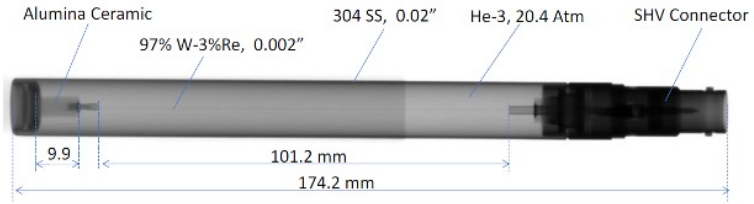

Figure 2.10: Computed tomography scans of the He-3 detectors that will be used to produce high-fidelity models for the final benchmark. Dimensions are in millimeters.

Figure 2.7: The Thermo Scientific P 383 neutron generator.

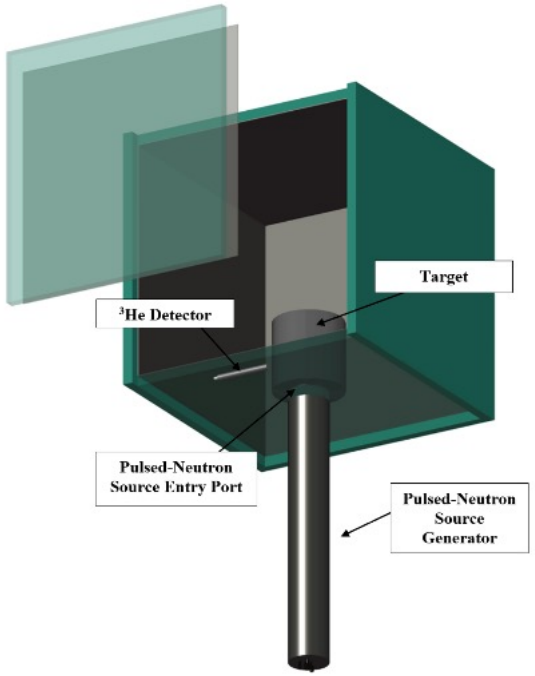

Figure 2.1: AutoCAD® rendering of the PNDA testbed (bottom view).

Subject of a later presentation by Dr. Daniel Siefman.

Questions? Comments?

Lawrence Livermore National Laboratory

Lawrence Livermore National Security, LLC
Operated for the US Department of Energy

P.O. Box 808, L-198

Livermore, CA 94551

David P Heinrichs

Division Leader

925-424-5679
Cell 925-667-1710
heinrichs1@llnl.gov

Nuclear Criticality Safety Division